Accepted for publication in Astrophysical Journal Letters
Preprint typeset using LaTeX style emulateapj v. 08/22/09

arXiv:1606.03526v1 [astro-ph.GA] 11 Jun 2016

AN ULTRALUMINOUS LYMAN ALPHA EMITTER WITH A BLUE WING AT Z=6.6 [1,2]

E. M. Hu [3], L. L. Cowie[3], A. Songaila[3], A. J. Barger[4,5,3], B. Rosenwasser[4], I. Wold[6]

Accepted for publication in Astrophysical Journal Letters

ABSTRACT

We report the detection of the most luminous high-redshift Lyman Alpha Emitting galaxy (LAE) yet seen, with $\log L(\mathrm{Ly}\alpha) = 43.9$ ergs s^{-1}. The galaxy – COSMOS Lyα1, or COLA1 – was detected in a search for ultraluminous LAEs with Hyper Suprime-Cam on the Subaru telescope. It was confirmed to lie at $z = 6.593$ based on a Lyα line detection obtained from followup spectroscopy with the DEIMOS spectrograph on Keck2. COLA1 is the first very high-redshift LAE to show a multi-component Lyα line profile with a blue wing, which suggests that it could lie in a highly ionized region of the intergalactic medium and could have significant infall. If this interpretation is correct, then ultraluminous LAEs like COLA1 offer a unique opportunity to determine the properties of the HII regions around these galaxies which will help in understanding the ionization of the $z \sim 7$ intergalactic medium.

Subject headings: cosmology: observations — galaxies: distances and redshifts — galaxies: evolution — galaxies: starburst

1. INTRODUCTION

The epoch of reionization is a key time in the evolution of the Universe, when the intergalactic medium (IGM) transitioned from being neutral to being very highly ionized. Determining when reionization occurred and finding the sources of the photons responsible is one of the major goals in current observational cosmology. Lyα emission is one of the few diagnostics of this epoch. Since it can be modified by the radiative damping wings of a neutral IGM, both the observed strength and the shape of the line are sensitive probes of the fraction of neutral hydrogen in the IGM (e.g. Haiman & Spaans 1999; Robertson et al. 2010). There is a developing consensus that the fraction of star-forming galaxies with Lyα emission (LAEs) drops rapidly from $z = 6$ to $z = 8$ (e.g. Stark et al. 2015; Treu et al. 2013; Tilvi et al. 2014; Schenker et al. 2014), which could reflect a rapid increase in the neutral hydrogen fraction in the IGM with increasing redshift.

However, theoretical modeling of the evolution of the LAE population is extremely difficult (e.g. Choudhury et al. 2015), and it is possible that this evolution may be driven by changes in the LAE properties of the galaxies as well as by IGM evolution (e.g. Stark et al. 2015). The galaxy itself produces a complex Lyα spectrum. At $z \sim 2-3$, Lyα lines generally have red offsets but in some 30% of cases show multi-component structures with blue wings (Kulas et al. 2012). The profiles can be crudely understood in terms of the velocity and structure of infalling and outflowing gas in the galaxy (e.g. Verhamme et al. 2012). At higher redshifts the IGM begins to modify the profiles (e.g. Dijkstra 2014). Beyond about $z \sim 4$ the Lyα forest begins to become optically thick (Songaila 2004) and will scatter the blue side of the Lyα line (and potentially some of the red side if there is infall of the IGM to the galaxy) out of the line of sight. This produces the asymmetric red profile that is characteristic of many of the LAEs. No multi-component LAE profiles are seen in the $z = 3-7$ LAE study of U et al. (2015) or in the $z = 5.7$ and $z = 6.6$ LAE samples of Hu et al. (2010) though there is wide variation in the degree of skewness in the lines. Multi-component structure can only be seen in $z >> 4$ galaxies if they highly ionize their surroundings and this is most likely for the most luminous galaxies. As the IGM becomes substantially neutral near reionization both the red and blue sides of the line will be suppressed by the radiative damping wings produced by the neutral part of the IGM lying outside the galaxy's HII region. The size of this effect depends on the neutral density in the surrounding IGM and also on the size of the HII region (Haiman 2002). In this case seeing the line at all depends on the formation of a large HII region and again this is more probable for the most luminous galaxies.

In the present paper we report the detection of the most luminous high-redshift LAE yet seen. This galaxy, which we call COSMOS Lyα 1 (COLA1), is the first high-redshift LAE ($z = 6.593$) to show a multi-component velocity structure with a blue wing, which suggests that COLA1 may indeed lie in a very highly ionized region of the IGM.

[1] Based on data collected at the Subaru Telescope, which is operated by the National Astronomical Observatory of Japan.

[2] The W. M. Keck Observatory is operated as a scientific partnership among the California Institute of Technology, the University of California, and NASA, and was made possible by the generous financial support of the W. M. Keck Foundation.

[3] Institute for Astronomy, University of Hawaii, 2680 Woodlawn Drive, Honolulu, HI 96822.

[4] Department of Astronomy, University of Wisconsin-Madison, 475 N. Charter Street, Madison, WI 53706.

[5] Department of Physics and Astronomy, University of Hawaii, 2505 Correa Road, Honolulu, HI 96822.

[6] Department of Astronomy, the University of Texas at Austin, 2515 Speedway Blvd., Stop C1400, Austin, TX 78712

2. DATA

We have been conducting a search for ultraluminous LAEs/faint AGN at $z = 6.6$ in six 4 deg^2 regions surrounding the COSMOS (158.082, 2.373), SSA22 (334.349, 0.2631), Lockman (160.033, 58.374), A370 (39.994, -1.586), CDF–S (53.123, -27.800), and CDF–N (189.22, 62.234) fields (central J2000 RA, Dec in decimal degrees in parentheses). In each case we have obtained deep g', i', z', and y' images with Hyper Suprime-Cam (HSC; Miyazaki et al. 2012) and narrow-band 9210 Å mosaicked images with Suprime-Cam, both on the Subaru telescope. The full data set and its implications for the behaviour of the bright end of the Lyα luminosity function will be described in Hu et al (2016; in preparation). Here we describe the data in the COSMOS field, the first field for which we have obtained complete spectroscopic follow-up with the Keck2/DEIMOS spectrograph.

The HSC observations of the COSMOS field were made with four overlapped HSC fields providing full coverage of an area with $\sim 2.1^\circ$ on a side. The data was obtained in March 2014 and January 2015. For each individual field we made two 5-point dither observations with an $11'$ throw. This was repeated in 4 orthogonal rotations (0,90,180,270) allowing removal of stellar diffraction spikes. We obtained observations in g' (31 min/pixel) i' (90 min, variable transmission) z' (30 min) and y' (85 min, variable transmission). Exposure times in the overlapped regions are larger. The seeing ranged from $0.75''$ in most of the z' band to $1.1 - 1.2''$ in the y'. The data was reduced with the HSC pipeline (http://hsca.ipmu.jp/public/pipeline/installation.html). The corresponding narrow-band observations were taken with the NB921 filter on the Suprime camera (center, 9183Å; FWHM, 132Å.) 144 fields were observed with a $10'$ step over 2 nights in Dec 2014. The total exposure per pixel was 900s. The observations were reduced with our standard pipeline (Capak et al. 2004), then combined into a single image, astrometrically matched to the HSC images. All narrow-band data was photometric with seeing $\sim 0.9''$.

We next formed a catalog of objects over the uniformly covered portions of the NB921 image to a limiting magnitude of NB921(AB)= 24.25 ($3''$ diameter aperture magnitude) corresponding to S/N $> 5\ \sigma$ throughout the area. The final narrow-band area coverage of 3 deg^2 is shown in the right panel of Figure 1, compared with the smaller narrow-band field of Sobral et al. (2015). We next searched for $z = 6.6$ LAE candidates with (z'-NB921)> 1 that were not detected above a 2σ level in g' and i'. The narrow-band and broad-band images of each of the candidates were next visually inspected and artifacts (moving objects, ghosts, and contamination by nearby bright objects) removed. All of the objects also lie within the Ultravista field and we also visually inspected the images of McCracken et al. (2012). We were left with a set of three objects, shown in Figure 1. Two of these, MASOSA, and CR7, were previously known and spectroscopically confirmed by Sobral et al. (2015) and Matthee et al. (2015). However COLA1, the most luminous of the three, lies outside the field observed by these authors (Figure 1). We compare the photometric properties of COLA1 and CR7 in Table 1 based on the present data. Both CR7 and COLA1 lie at the long-wavelength edge of the NB921 filter and we must allow for the falling transmission in the filter when converting the narrow-band magnitude to a flux. Allowing for the relative transmission factors, the imaging data shows COLA1 to be about 20% more luminous than CR7.

TABLE 1
Properties of COLA1 and CR7

	COLA1	CR7
Photometric		
g'	$27.26^{28.05}_{26.82}$	$-27.42^{-28.38}_{-26.82}$
i'	$27.10^{29.04}_{26.44}$	$-27.38^{-30.17}_{-26.59}$
z'	$25.39^{26.08}_{24.97}$	$25.51^{26.33}_{25.04}$
NB921	$23.50^{23.60}_{23.41}$	$23.86^{24.01}_{23.73}$
y'	$25.10^{25.53}_{24.79}$	$24.71^{25.00}_{24.48}$
Spectroscopic		
z(Lyα)	6.593	6.605
$\log L$(Lyα) (erg s^{-1})	43.9	43.8
FWHM(Lyα) (km s^{-1})	194	247
EW(Lyα) (Å)	53	99

$3''$ diameter aperture magnitudes, flux-calibrated by comparison with the COSMOS magnitudes of Capak et al. (2007) in the overlapping region. A minus sign denotes negative flux in the aperture and the number corresponds to the absolute value of the flux. 1 σ errors in the band were determined by measuring the dispersion in blank field positions with the same aperture, and are NB921 26.1, y' 26.3, z' 26.2, i' 27.3 and g' 28.0, close to the predicted noise. The 1 σ range for each magnitude is shown with the upper and lower subscripts.

We observed COLA1 with the Keck2/DEIMOS spectrograph on March 6th 2016, with the G830 grating using a $1''$ slit, giving a resolution measured from the sky lines of 83 km s^{-1} for the $z = 6.6$ LAEs. Three 20-min exposures were obtained, dithered by $\pm 1.5''$ along the slit, to obtain precise sky subtraction. The seeing was $0.6''$ and conditions were photometric. The data was reduced with our standard pipeline (Cowie et al. 1996). For detailed comparison with COLA1, we also observed CR7 in the same configuration but we did not re-observe the fainter MASOSA. The 2-D spectra of COLA1 and CR7 are shown in Figure 2, compared with two of the most luminous LAEs from Hu et al. (2010). In Figure 3, we compare the line profile of COLA1 with that of CR7 and also with the stacked spectra of lower-luminosity LAEs at $z = 6.6$ from Hu et al. (2010) with luminosities, $\log L(\mathrm{Ly}\alpha) < 43.3$ ergs^{-1}.

The optical spectroscopic follow-up shows that COLA1 lies at a redshift of 6.593 based on the peak of the Lyα profile. However, more surprisingly, it has a complex line profile with both blue and red components. The flux of COLA1 is 1.4 times that of CR7 based on the spectroscopy. Even excluding the blue wing, COLA1 is still more luminous than CR7, so the selection of COLA1 is not biased by its unique profile. Indeed, the shape of the red wing is almost identical in the two galaxies and almost indistinguishable from the stack of lower-luminosity

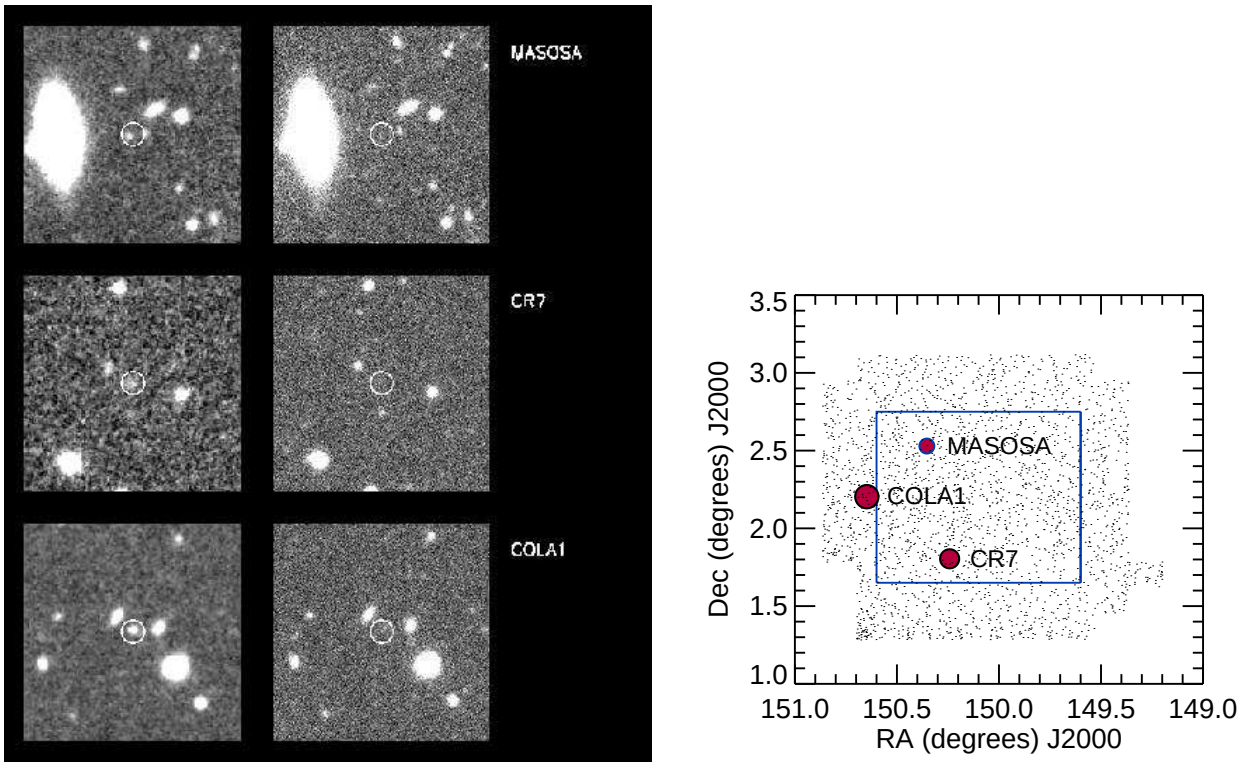

FIG. 1.— *Left*: Images (left – NB921, right – z') of the three brightest LAEs in our extended COSMOS field. The LAE is circled in each image. Thumbnails are 30″ on a side. All three galaxies are physically extended. COLA1 has an angular size of $\sim 0.2''$. *Right*: Location of these objects in the region around the COSMOS field (red circles). The black shading shows the region covered by the present narrow-band observations while the blue square shows the approximate region covered by Sobral et al. (2015). COLA1 lies outside this latter region.

line profiles given in Hu et al. (2010) (Figure 3).

The measured FWHM, corrected for the instrumental resolution, is 194 km s^{-1} in COLA1 compared to 247 km s^{-1} in CR7. (Sobral et al. (2015) give a Gaussian-fitted FWHM of 266±15 km s^{-1} for CR7.) Only the red side of COLA1 lies above the half maximum so the FWHM relates to this component only. The measured rest-frame equivalent width of COLA1 is 53Å and that of CR7 99Å, where in both cases we have measured the continuum to redward of the line. Both MASOSA and COLA1 are quite spatially compact. In the narrow-band image COLA1 has a measured FWHM of 0.93″ compared with the locally measured PSF of $0.88 \pm 0.02''$ giving an intrinsic FWHM of 0.3″. In $y\prime$ the local PSF is $0.77 \pm 0.01''$ and the COLA1 FWHM is 0.90″ giving an intrinsic FWHM of 0.46″. This contrasts with CR7 which is quite diffuse (Sobral et al. 2015). The present data gives an intrinsic FWHM of 1.3″ for CR7. There is no sign of any N V 1240 Å emission though this lies in a noisier part of the spectrum where there are strong night sky lines.

At lower redshifts ($z = 2.2$) Konno et al. (2015) suggest that almost all Lyα emitters with $L(\mathrm{Ly}\alpha) > 10^{43.4}$ ergs^{-1} are associated with AGN. However, the narrowness of the Lyα line (see Alexandroff et al. 2013; Matsuoka et al. 2016) the spatial extension of the galaxy and the absence of N V 1240Å (though the latter two constraints are weak) combine to suggest that COLA1 is primarily powered by star formation rather than AGN activity. However, both COLA1 and CR7 could have AGN contributions to their emission.

3. PHYSICAL INTERPRETATION

It seems, therefore, that the most luminous LAE ever detected in the epoch of reionization has a unique and unexpected line profile. The simplest explanation for this surprising result is that COLA1 lies in a highly ionized region of gas, increasing the Lyα forest transmission and thereby allowing us to see the blue side of the Lyα line profile. Alternatively, the galaxy could be moving at a velocity of several hundred km s^{-1} with respect to the IGM, so that the Lyα profile has been moved redward of the effects of IGM scattering. The compactness of the galaxy and the spatial alignment of the blue and red wings in the 2-D spectrum makes it unlikely the velocity structure is caused by a galaxy merger.

Matthee et al. (2015) have argued that there is little evolution in the luminosity function of the most luminous LAEs at these redshifts, suggesting that these objects lie in large HII regions and protect themselves from any changes in IGM neutrality. This would be consistent with complex Lyα profiles being seen only in the most ultraluminous LAEs.

At low redshifts ($z = 2 - 3$) about 30% of LAEs show multi-component profiles (Kulas et al. 2012). Kulas et al. argue that these galaxies are not strongly affected by IGM opacity so that this fraction could also be applicable to the high-redshift galaxies enclosed in giant HII regions (though of course the properties of the high-redshift galaxies may be very different). Assuming that COLA1, CR7 and MASOSA lie in this class then we do indeed see one galaxy in three having a complex profile, which would be crudely consistent. If this is the cor-

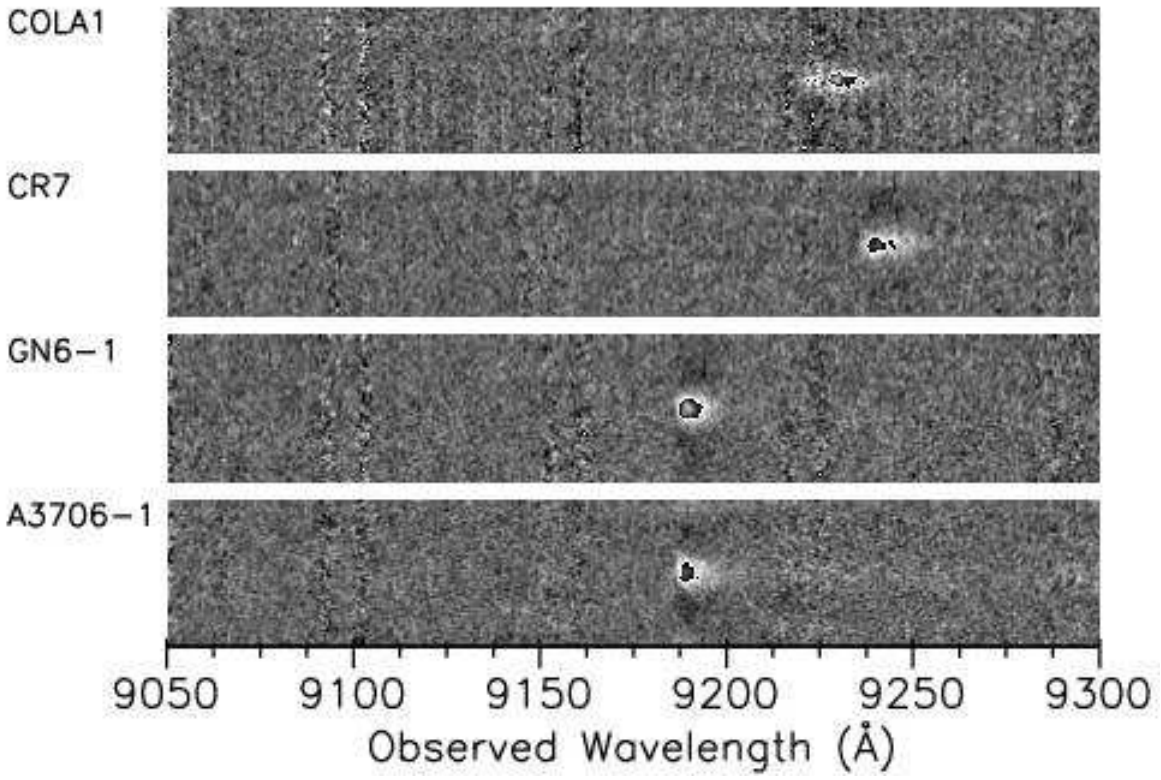

FIG. 2.— Two-dimensional spectral images of COLA1 (top) and CR7 (middle) compared with the brightest $z = 6.6$ LAE in the GOODS-N (GN6-1) and A370 (A3706-1) fields of Hu et al. (2010) (bottom).

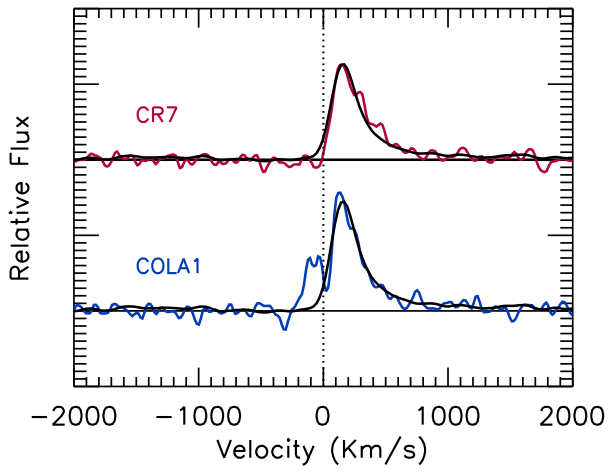

FIG. 3.— Spectra of the two most ultraluminous LAEs. *Bottom*: COLA1 *Top*: CR7. CR7's velocity is in the reference frame of the galaxy's HeII line, giving peak Lyα at 160 km s^{-1}. COLA1 is plotted with the peak at the same offset. Under this assumption the blue side extends to ~ -200 km s^{-1}. Both objects also show a continuum break across the line. The black overlay shows the composite $z = 6.6$ LAE profile of Hu et al. (2010) normalized to match the maximum in each of the objects.

rect interpretation, then more complex profiles may be present in a fraction of the most ultraluminous LAEs.

COLA1's velocity structure appears very similar to that of multicomponent LAEs at lower redshift though with lower velocities (e.g. Kulas et al. 2012; Quider et al. 2010). The peak in the blue side has a maximum that is 0.44 times that of the red side and the velocity separation between the red and blue peaks is 215 km s^{-1}. Our assumed velocity offset places the trough between the peaks at 25 km s^{-1}, close to the near-zero velocity seen in most low-redshift LAEs in Kulas et al. (2012).

As discussed in §1, interpreting the LAE profiles is complicated (e.g. Verhamme et al. 2012). The velocity separation of the peaks and the redside velocity can be produced with an expanding shell with a velocity of $\sim$ 50 km s^{-1} but such a model would predict a much stronger red-to-blue ratio than is seen in COLA1, suggesting we also need significant infall. We postpone more detailed discussion until an an exact determination of the absolute velocity scale is obtained. However, if COLA1 does have a strong inflow this might suggest that the galaxy is in an early formation phase and has a low metallicity. This would be consistent with the Sobral et al. (2015) interpretation of CR7 as having a young, metal-poor stellar population.

If we accept that the complex line's visibility is a result of HII region ionization, then we may be able to draw useful inferences about the IGM and the escape of ionizing photons from the galaxy. Unfortunately the reduction in the Lyα flux and the scattering of the blue side by the presence of the HII region depend on a very large num-

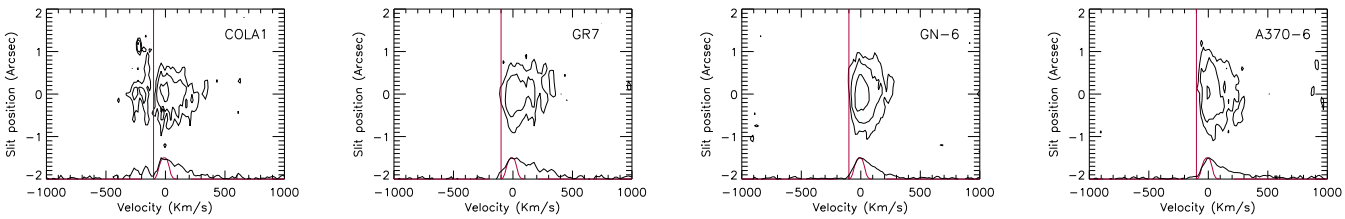

FIG. 4.— Two-dimensional spectra of the LAEs. Lyα luminosity decreases from left to right. COLA1 ($\log L(\mathrm{Ly}\alpha) = 43.9$ erg s^{-1}) shows a clear blue extension, CR7 ($\log L(\mathrm{Ly}\alpha) = 43.8$ erg s^{-1}) does not show a clear sharp velocity edge, and the two lower luminosity objects (GN-6 with $\log L(\mathrm{Ly}\alpha) = 43.3$ erg s^{-1}) and A370-6 with $\log L(\mathrm{Ly}\alpha) = 43.2$ erg s^{-1}) show the sharp razor-edge cutoff typical of lower-luminosity objects at this redshift. In all cases the zero velocity is shown at the Lyα peak and the vertical red line marks -100 km s^{-1}. The contours drop by a multiplicative factor of two. At the bottom we show the line profile (black) and the spectral resolution profile (red) centered at 0 km s^{-1}.

ber of parameters. The HII region size depends on the total number of ionizing photons from the galaxy and inversely on x_{IGM}, the IGM neutral hydrogen fraction. Haiman (2002) gives the size as

$$R_S = 0.45\, x_{\mathrm{IGM}}^{-1/3} \left(\frac{N_{ion}}{5\times10^{69}}\right)^{1/3} \mathrm{Mpc}\ . \qquad (1)$$

Here R_s is in proper Mpc and N_{ion} is the total number of ionizing photons released by the galaxy. N_{ion} depends on the star-formation rate of the galaxy, its initial mass functions, the ionizing photon escape fraction (f_{esc}), and the age of the galaxy. It is correspondingly an extremely uncertain quantity. Nevertheless, the HII region radius is generally large enough that we can largely ignore the effects on the Lyα line of the radiation damping wings of the IGM outside the HII region unless the IGM is substantially neutral (Miralda-Escudé 1998; Haiman 2002).

In this case the amount of scattering in the Lyα profile is dependent only on the residual density of neutral gas in the HII region (Haiman 2002; Haiman & Cen 2005). This affects only the blue side of the profile where the gas lies at lower redshifts than the galaxy. The fractional neutral hydrogen in the HII region is given by Cen & Haiman (2000) as

$$x_{\mathrm{HII}} = 8\times10^{-4} C_{\mathrm{HII}} \left(\frac{r}{\mathrm{Mpc}}\right)^2 \left(\frac{\dot{N}_{ion}}{10^{54}\ \mathrm{s}^{-1}}\right)^{-1}\ . \qquad (2)$$

Here C_{HII} is the clumping factor, r is the radial distance from the galaxy, and $\dot{N}_{ion}$ is the rate at which the galaxy releases ionizing photons into the IGM. Translated simply, this predicts a large optical depth even for relatively low values of $\dot{N}_{ion}$. Haiman (2002) has values of τ_{HII} near 100 for $\dot{N}_{ion} \sim 10^{54}$ s^{-1}, characteristic of a moderate luminosity LAE with a high escape fraction. However, the effects of structure must be taken into account since the transmission is dominated by lower-density regions and this significantly reduces the effective optical depth. With plausible assumptions, Haiman (2002) showed that this effect reduces the optical depth by almost three orders of magnitude, placing an optical depth of one on the immediate blue side of the LAE for a galaxy with this value of $\dot{N}_{ion}$. Thus it is plausible that a change in the LAE properties occurs when $\dot{N}_{ion}$ rises significantly above 10^{54} s^{-1} and the HII region becomes effectively thin. If we assume this change occurs at around the Lyα luminosity of MASOSA ($\log L(\mathrm{Ly}\alpha) = 43.4$; Sobral et al. 2015) we can convert this to an ionizing photon release of $\sim 1.6\times10^{46} f_{\mathrm{esc}}$, assuming the case B conversion to $L(\mathrm{H}\alpha)$ and a Salpeter IMF (e.g. Matthee et al. 2015). The two match for $f_{\mathrm{esc}} \sim 0.01$ but the significant uncertainties in the computation of the optical depth arising from the HII region must be borne in mind.

If this is correct we would expect to see a change in the structure of the lines at the transition point. Below the critical $\dot{N}_{ion}$ the effects of HII absorption should produce a sharp razor-edge cutoff at all positions on the galaxy, as indeed is seen in the lower-luminosity LAEs (Figure 4) where the cutoff essentially corresponds to the instrument profile. At higher luminosities the cutoff is just due to the profile emerging from the galaxy and can show variation across the galaxy, as is seen in both COLA1 and CR7.

4. SUMMARY

The discovery of COLA1 at $z = 6.593$ — the most luminous LAE ever detected near the reionization epoch and the highest redshift LAE to show a multi-component structure with a blue wing – has the potential to significantly improve our understanding of the ionization of the IGM by galaxies at $z = 6.6$. We suggest that the most luminous LAEs lie in HII regions which are sufficiently highly ionized by the galaxy to allow unscattered transmission of the blue side of the Lyα line. The transition Lyα luminosity at which this occurs allows an estimate of the escape fraction of ionizing photons from the galaxy. If this interpretation is correct then a substantial number of the most ultraluminous LAEs may show complex line profiles, and modeling of the profiles should allow us to determine the kinematic structure of the galaxies. Large samples of ultraluminous LAEs should soon be available from wide-field surveys with HSC on Subaru and should allow us to study these issues in detail.

We gratefully acknowledge support from NSF grants AST-1313309 (L. L. C.) and AST-1313150 (A. J. B) and the University of Wisconsin Research Committee with funds granted by the Wisconsin Alumni Research Foundation (A. J. B.). We would like to thank John Silverman and Guenther Hasinger for providing the reductions of

the HSC data on the COSMOS field and Zoltan Haiman and the anonymous referee for their reviews of the first draft of the manuscript. We acknowledge the cultural significance that the summit of Mauna Kea has for the indigenous Hawaiian community.

REFERENCES

Alexandroff, R., Strauss, M. A., Greene, J. E., et al. 2013, MNRAS, 435, 3306
Capak, P., Cowie, L. L., Hu, E. M., et al. 2004, AJ, 127, 180
Capak, P., Aussel, H., Ajiki, M., et al. 2007, ApJS, 172, 99
Cen, R., & Haiman, Z. 2000, ApJ, 542, L75
Choudhury, T. R., Puchwein, E., Haehnelt, M. G., & Bolton, J. S. 2015, MNRAS, 452, 261
Cowie, L. L., Songaila, A., Hu, E. M., & Cohen, J. G. 1996, AJ, 112, 839
Dijkstra, M. 2014, PASA, 31, e040
Haiman, Z. 2002, ApJ, 576, L1
Haiman, Z., & Cen, R. 2005, ApJ, 623, 627
Haiman, Z., & Spaans, M. 1999, ApJ, 518, 138
Hu, E. M., Cowie, L. L., Barger, A. J., et al. 2010, ApJ, 725, 394
Konno, A., Ouchi, M., Nakajima, K., et al. 2015, ArXiv e-prints, arXiv:1512.01854
Kulas, K. R., Shapley, A. E., Kollmeier, J. A., et al. 2012, ApJ, 745, 33
Matsuoka, Y., Onoue, M., Kashikawa, N., et al. 2016, ArXiv e-prints, arXiv:1603.02281
Matthee, J., Sobral, D., Santos, S., et al. 2015, MNRAS, 451, 400
McCracken, H. J., Milvang-Jensen, B., Dunlop, J., et al. 2012, A&A, 544, A156
Miralda-Escudé, J. 1998, ApJ, 501, 15
Miyazaki, S., Komiyama, Y., Nakaya, H., et al. 2012, in Proc. SPIE, Vol. 8446, Ground-based and Airborne Instrumentation for Astronomy IV, 84460Z
Quider, A. M., Shapley, A. E., Pettini, M., Steidel, C. C., & Stark, D. P. 2010, MNRAS, 402, 1467
Robertson, B. E., Ellis, R. S., Dunlop, J. S., McLure, R. J., & Stark, D. P. 2010, Nature, 468, 49
Schenker, M. A., Ellis, R. S., Konidaris, N. P., & Stark, D. P. 2014, ApJ, 795, 20
Sobral, D., Matthee, J., Darvish, B., et al. 2015, ApJ, 808, 139
Songaila, A. 2004, AJ, 127, 2598
Stark, D. P., Richard, J., Charlot, S., et al. 2015, MNRAS, 450, 1846
Tilvi, V., Papovich, C., Finkelstein, S. L., et al. 2014, ApJ, 794, 5
Treu, T., Schmidt, K. B., Trenti, M., Bradley, L. D., & Stiavelli, M. 2013, ApJ, 775, L29
U, V., Hemmati, S., Darvish, B., et al. 2015, ApJ, 815, 57
Verhamme, A., Dubois, Y., Blaizot, J., et al. 2012, A&A, 546, A111